Optimization and Engineering manuscript No.
(will be inserted by the editor)

Bilevel optimal control of urban traffic-related air pollution by means of Stackelberg strategies

N. García-Chan · L.J. Alvarez-Vázquez · A. Martínez · M.E. Vázquez-Méndez

Received: date / Accepted: date

Abstract Air contamination and road congestion are two major problems in modern cities. Both are closely related and present the same source: traffic flow. To deal with these problems, governments impose traffic restrictions preventing the entry of vehicles into sensitive areas, with the final goal of decreasing pollution levels. Unfortunately, these restrictions force drivers to look for alternative routes that usually generate traffic congestions, resulting in longer travel times and higher levels of contamination. In this work, blending computational modelling and optimal control of partial differential equations, we formulate and analyse a bilevel optimal control problem with air pollution and drivers' travel time as objectives and look for optimal solutions in the sense of Stackelberg. In this setting, the leader (local government) implements traffic restrictions meanwhile the follower (drivers set) acts choosing travel preferences against leader constraints. We discretize the problem and propose a numerical algorithm to solve it, combining genetic-elitist algorithms and interior-point methods. Finally, computational results for a realistic case posed in the Guadalajara Metropolitan Area (Mexico) are shown.

Keywords Bilevel optimization · Numerical simulation · Optimal control · Stackelberg solution · Traffic-related air pollution

N. García-Chan
Depto. Física, Universidad de Guadalajara, C.U. Ciencias Exactas e Ingenierías, 44430 Guadalajara, México
E-mail: nestor.gchan@academicos.udg.mx

L.J. Alvarez-Vázquez · A. Martínez
Depto. Matemática Aplicada II, Universidade de Vigo, E.I. Telecomunicación, 36310 Vigo, Spain
E-mail: lino@dma.uvigo.es; aurea@dma.uvigo.es

M.E. Vázquez-Méndez
Depto. Matemática Aplicada, Universidade de Santiago de Compostela, E.P.S., 27002 Lugo, Spain
E-mail: miguelernesto.vazquez@usc.es

Mathematics Subject Classification (2010) 90C29 · 90B50 · 49J20

1 Introduction

Expansive growth of big cities all around the world has originated, as an undesirable collateral effect, the critical increasing of two closely related environmental problems: traffic congestion and air pollution, whose main factor can be considered urban traffic. Regarding the first problem, the main negative consequences are related to the increase in the necessary time for its residents to carry out their daily moves, with the resulting discomfort associated, for instance, with excessive fuel consumption, delays and noise pollution. For the second problem, urban atmospheric contamination is highly subordinate to vehicular emissions (carbon oxides, nitrogen oxides and so on), but concentration levels of such pollutants depend also on other external factors such as, among others, wind or humidity.

To confront these problems, common public policies imposed by the local governments are related to traffic restrictions at the intersections of the urban road network. With these restrictions, they prevent the entry of vehicles into sensitive areas (normally the city center) with the aim of bringing down the air pollution concentration. However, these limitations force drivers to choose other road preferences to reach their destiny, inducing traffic congestions. Thus, contrary to expectations, these traffic congestions can increase pollutant concentrations and present a negative impact on drivers with longer travel times.

The reduction of air pollution levels by the traffic restrictions and their consequent change in drivers' preferences, is nowadays a controversial topic. Recent studies show that the impact of the traffic restrictions (and other traffic management strategies) on air pollution levels are moderately successful in low emissions zones of some European cities. Meanwhile, the lack of data and the complexity of epidemiology studies made harder the detection and identification of traffic-related health impact on inhabitants by exposure to noise, stress and air pollution (see Bigazzia and Rouleau (2017) and the references therein). However, studies also showed that this impact on air pollution can be greater and that society is aware of the need of these traffic restrictions policies. In Invernizzi et al. (2011) the concentration of black carbon was compared with the concentration of particulate matter (PM) in three zones of Milan (Italy): without traffic restrictions, with traffic restrictions and for pedestrians only. This data analysis showed (roughly speaking) that the concentration levels of black carbon drop down from traffic areas to pedestrian areas meanwhile, the PM concentration does it but in a more moderate way. In Pestana-Barros and Dieke (2008) an inquest to the inhabitants of Lisbon (Portugal) showed that they are willing to accept charges for vehicular congestions with the aim of a better quality of life.

Those studies Invernizzi et al. (2011) and Bigazzia and Rouleau (2017) are mainly empirical, and *a priori* evaluation or even the certainty of dropping

down the air pollution levels by traffic restrictions are out of their point of view. Therefore, a suitable combination of mathematical models, numerical simulation and optimal control techniques are an important tool for estimating and optimizing the impact of traffic restrictions and drivers' preferences on the air pollution levels and the drivers' travel times. Moreover, these *a priori* estimates and minimization results could be employed as a factor to change the viewpoint of city inhabitants, making them agree to these traffic management policies.

Within this context, partial differential equations models are usually employed both in the analysis of urban traffic flow in road networks (Coclite at al. (2017), Garavello and Piccoli (2009); Garavello et al. (2016); Goatin et al. (2016); Goettlich et al. (2015); Holden and Risebro (1995)) and in the investigation of atmospheric pollution (Alvarez-Vázquez et al. (2015a); García-Chan et al. (2014); Orun et al. (2018); Skyba and Parra-Guevara (2013); Stockie (2011)). Nevertheless, the compounding of both topics has been much less addressed (we can mention, for instance, Berrone et al. (2012); Canic et al. (2015); García-Chan et al. (2017); Gottlich et al. (2011); Parra-Guevara and Skyba (2003)) , and is usually based on the assumption of previous knowledge of the vehicular flow, which is not adapted to analyze the management of a road network that may be optimal to travel times and contamination levels.

The authors have addressed this topic in a series of recent works with progressive complexity. So, in Alvarez-Vázquez et al. (2017) a new methodology that couples a 1D model for vehicular flow with a 2D model for pollutant dispersion was proposed, to estimate the air pollution related to traffic flow. In Alvarez-Vázquez et al. (2018) an optimal control problem related to the expansion of an existing urban road network with an environmental perspective was formulated and solved. Finally, in Vázquez-Méndez et al. (2019) a multiobjective optimal control problem -where the air pollution and the travel time were the objectives, the drivers' preferences were the controls, and the traffic restrictions were fixed- was solved from a cooperative point of view, that is, its Pareto front was obtained using a genetic algorithm.

Thus, within the framework of optimal control of partial differential equations, the current work represents a forward step in the same direction, now analysing and solving -and this is the main contribution of this research- a novel formulation from a non-cooperative, hierarchical point of view, that is, a Stackelberg strategy (Stackelberg (1952)), which seems a more realistic option for this real-world scenario. Stackelberg strategies are commonly applied in economy (Julien and Tricou (2012)), and the authors have previously employed them in the optimal management of a wastewater system (Alvarez-Vázquez et al. (2015b)). Therefore, in the present context of minimizing the urban air pollution levels and the drivers' travel time, the existence of a hierarchical relation between the local government (denoted as the leader) and the set of drivers (denoted as the follower) is considered. Concerning the follower, we assumed that drivers are cooperating among them to reduce their travel time against to leader's decision, despite individual driver's interest. This cooperative driving is a necessary quality in the driver behavior models and possibly achievable

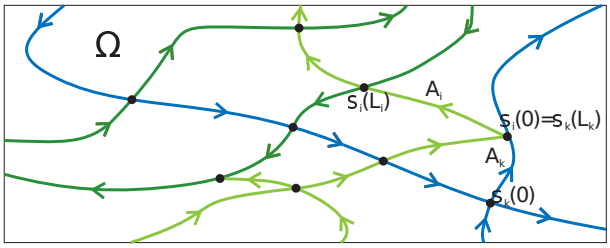

Fig. 1 Scheme of a typical domain Ω corresponding to a city with a road network

with a social conscience and the use of technology (AbuAli and Abou-Zeid (2016); Mertens et al. (2020); Shahab (2012)). So, a bilevel optimal control problem is formulated and its Stackelberg solution is formally defined (Section 3). Then, a complete discretization of the cost functionals and a combination of an interior-point method (Waltz et al. (2006)) with a genetic-elitist algorithm (Deb (2000); Goldberg (2016)) is proposed to solve this bilevel problem. This combination is carried out using adjoint state techniques (Marchuk (1986)), where the pollutant objective functional is written in an alternative, simpler way (that considers the adjoint state and the pollutant emissions both only evaluated on the road network instead of the pollution state evaluated in the whole urban domain), to reduce the computational cost (Section 4). Finally, some numerical experiences for a real-world case posed in one of the largest metropolitan areas in Mexico (the Guadalajara Metropolitan Area (GMA), with almost five million inhabitants and more than two million vehicles) are presented (Section 5), and several concluding remarks are derived (Section 6).

2 Mathematical modelling

Let $\Omega \subset \mathbb{R}^2$ be a domain representing a city, including an urban road network formed by N_R unidirectional avenues crossing at N_J intersections, and such that each road endpoint is either an intersection or lies on the boundary of Ω (see a schematic example in Fig. 1).

Each avenue $A_i \subset \Omega,\ i = 1, \ldots, N_R$, is represented by an interval $[0, L_i]$ parametrized by means of the horizontal alignment $\sigma_i : s \in [0, L_i] \subset \mathbb{R} \longrightarrow \sigma_i(s) = (x_i(s), y_i(s)) \in A_i$, where the arc length parameter s preserves the sense of motion on the road. In the following, we denote by $\mathcal{I}^{in}, \mathcal{I}^{out} \subset \{1, \ldots, N_R\}$ the sets of indices designating incoming and outgoing avenues in the network, respectively, and by $\mathcal{I}_j^{in}, \mathcal{I}_j^{out} \subset \{1, \ldots, N_R\}$ the sets of indices designating incoming and outgoing avenues at the intersection $j \in \{1, \ldots, N_J\}$, respectively.

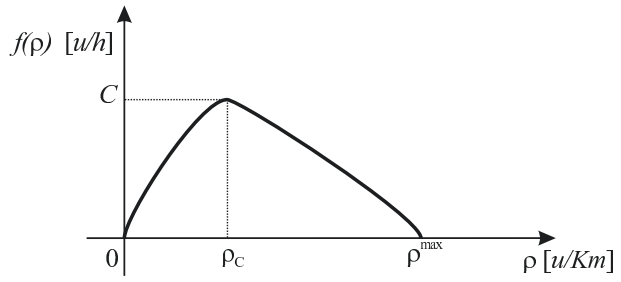

Fig. 2 Classical static relation showing flow rate $f(\rho) = \rho v$ versus density ρ, and depicting maximum density ρ^{max}, critical density ρ_C and road capacity C

2.1 Modelling traffic flow

In whole road network, traffic flow is modelled by the classical Lighthill-Whitham-Richards (LRW) model coupled with queue terms. Then, we denote by $\rho_i(s,t) \in [0, \rho_i^{max}]$ the density of cars at point $\sigma_i(s)$ of avenue A_i and at time $t \in [0,T]$ (measured in number of cars/km), where ρ_i^{max} represents the maximum allowed density. The LRW model assumes that the flow rate on each avenue A_i [number of cars/h] is given by a function $f_i : [0, \rho_i^{max}] \to \mathbb{R}$ in terms of the density (i.e., $f_i(\rho_i) = \rho_i v_i$, where v_i [km/h] represents the velocity on the avenue A_i). Fundamental diagram f_i is usually known as the *static relation* on A_i (see Fig. 2), and its main properties can be found, for instance, in Vázquez-Méndez et al. (2019).

Moreover, for all $y \in \mathcal{I}^{in}$, we define the queue length $q_y(t) \geq 0$ (measured in *number of cars*) downstream the avenue A_y, where we assume known the desired inflow rate $f_y^{in}(t)$ and the downstream road capacity C_y^{in}. We also suppose that, for all $z \in \mathcal{I}^{out}$, the maximum outflow rates $f_z^{out}(t)$ are given.

So, traffic flow in the whole road network is defined by the solution of the following system (Garavello et al. (2016); Vázquez-Méndez et al. (2019)): for $i = 1, \ldots, N_R$, $y \in \mathcal{I}^{in}$, $z \in \mathcal{I}^{out}$, $j = 1, \ldots, N_J$, $k \in \mathcal{I}_j^{in}$, and $l \in \mathcal{I}_j^{out}$:

$$\frac{\partial \rho_i}{\partial t} + \frac{\partial f_i(\rho_i)}{\partial s} = 0 \quad \text{in } (0, L_i) \times (0,T), \quad \text{(1a)}$$

$$\rho_i(.,0) = \rho_i^0 \text{ in } [0, L_i], \quad \text{(1b)}$$

$$f_k(\rho_k(L_k,.)) = \sum_{l \in \mathcal{I}_j^{out}} \min\left\{\alpha_{lk}^j D_k(\rho_k(L_k,.)),\, \beta_{kl}^j S_l(\rho_l(0,.))\right\} \text{ in } (0,T), \quad \text{(1c)}$$

$$f_l(\rho_l(0,.)) = \sum_{k \in \mathcal{I}_j^{in}} \min\left\{\alpha_{lk}^j D_k(\rho_k(L_k,.)),\, \beta_{kl}^j S_l(\rho_l(0,.))\right\} \text{ in } (0,T), \quad \text{(1d)}$$

$$f_z(\rho_z(L_z,.)) = \min\{f_z^{out}, D_z(\rho_z(L_z,.))\} \quad \text{in } (0,T), \quad \text{(1e)}$$

$$f_y(\rho_y(0,.)) = \min\{D_y^{in}(q_y,.), S_y(\rho_y(0,.))\} \quad \text{in } (0,T), \quad \text{(1f)}$$

$$\left.\begin{array}{l} \dfrac{dq_y}{\mathrm{d}t} = f_y^{in} - f_y(\rho_y(0,.)) \text{ in } (0,T), \\ q_y(0) = q_y^0, \end{array}\right\} \tag{1g}$$

where terms D_i and S_i represent the demand and supply functions respectively, and term $D_y^{in}(q_y,t)$ represents the demand of queue q_y at time t (Alvarez-Vázquez et al. (2017); Vázquez-Méndez et al. (2019). Furthermore,

* array $\boldsymbol{\alpha} = (\alpha_{lk}^j)$ stands for drivers' preferences when arriving at a junction, i.e., α_{lk}^j represents the rate of drivers that, reaching intersection j coming from road A_k, will take the outgoing road A_l. Thus, the following compatibility constraints need to be verified:

$$0 \leq \alpha_{lk}^j \leq 1 \quad \text{and} \quad \sum_{l \in \mathcal{I}_j^{out}} \alpha_{lk}^j = 1. \tag{2}$$

* array $\boldsymbol{\beta} = (\beta_{kl}^j)$ stands for ingoing capacities at outgoing roads, i.e., β_{kl}^j represents the rate of vehicles that, arriving at junction j for road A_k, can enter the outgoing road A_l. As above, these parameters should satisfy:

$$0 \leq \beta_{kl}^j \leq 1 \quad \text{and} \quad \sum_{k \in \mathcal{I}_j^{in}} \beta_{kl}^j = 1. \tag{3}$$

We have to mention here that these arrays will be the design variables for our bilevel problem. Finally, it is also worthwhile recalling the fundamental role of coupling conditions (1c) and (1d) -depending strongly on arrays $\boldsymbol{\alpha}$ and $\boldsymbol{\beta}$- to guarantee the conservation of the number of cars at intersections.

2.2 Modelling atmospheric pollution

Traffic-related air pollution is simulated here by a mathematical model similar to the one proposed in Alvarez-Vázquez et al. (2018), whose uniqueness of solution was analysed in Casas (1997) and Martínez et al. (2017). Due to its main role, we focus our interests only in pollution related to nitrogen oxides (NO_x), but many other kinds of pollution -like carbon oxides (CO_x), sulphur oxides (SO_x), total hydrocarbons (THC), etc.- could be also included. The choice of the type of pollution to be controlled depends on the particular characteristics of the region under study (for instance, NO_x emissions are more related to diesel engines, whereas on-road CO_x is more associated with gasoline engines). So, in our case, the NO_x concentration $\phi(x,t)$ $[kg/km^2]$ corresponding to each point $x \in \Omega$ and each time $t \in [0,T]$, can be obtained

by solving the following initial/boundary value problem:

$$\frac{\partial \phi}{\partial t} + \mathbf{v} \cdot \nabla \phi - \nabla \cdot (\mu \nabla \phi) + \kappa \phi = \sum_{i=1}^{N_R} \xi_{A_i} \quad \text{in } \Omega \times (0,T), \tag{4a}$$

$$\phi(.,0) = \phi^0 \quad \text{in } \Omega, \tag{4b}$$

$$\mu \frac{\partial \phi}{\partial n} - \phi\, \mathbf{v} \cdot \mathbf{n} = \sum_{y \in \mathcal{I}^{in}} \lambda_y q_y \delta_{\sigma_y(0)} \quad \text{on } S^-, \tag{4c}$$

$$\mu \frac{\partial \phi}{\partial n} = 0 \quad \text{on } S^+, \tag{4d}$$

where field $\mathbf{v}(x,t)$ [km/h] denotes wind velocity, and vector $\mathbf{n}$ denotes the unit outward normal vector to the boundary $\partial\Omega = S^- \cup S^+$, split into the outflow boundary $S^+ = \{(x,t) \in \partial\Omega \times (0,T) \text{ such that } \mathbf{v} \cdot \mathbf{n} \geq 0\}$ and the inflow boundary $S^- = \{(x,t) \in \partial\Omega \times (0,T) \text{ such that } \mathbf{v} \cdot \mathbf{n} < 0\}$. Second member terms ξ_{A_i} [kg/km^2/h] represent pollution sources due to vehicular traffic on roads A_i, and are given by means of a Radon measure: for each $t \in [0,T]$, the distribution $\xi_{A_i}(t) : \mathcal{C}(\overline{\Omega}) \longrightarrow \mathbb{R}$ is defined by:

$$\langle \xi_{A_i}(t), v \rangle = \int_0^{L_i} \left(\gamma_i f_i(\rho_i(s,t)) + \eta_i \rho_i(s,t)\right)\, v(\sigma_i(s))\, ds, \quad \forall v \in \mathcal{C}(\overline{\Omega}),$$

where σ_i is the parametrization of avenue A_i, density ρ_i is given by the traffic model (1), and parameters γ_i and η_i are weights associated to pollution rates. Further details on coefficients can be found in Vázquez-Méndez et al. (2019).

3 A bilevel non-cooperative optimal control problem

In previous approaches to traffic management in a road network, standard objectives were usually related only to traffic problems, such as travel time or congestions. Nevertheless, present-day difficulties with air pollution in the surroundings of big metropolises have turned the mitigation of this phenomenon into another major aim in the optimal management of urban road networks. Here, two different objectives, one of each type, will be considered simultaneously. Concerning optimizing the traffic flow, it is important to minimize the total travel time and to maximize the outflow of the network. In the spirit, for instance, of Goatin et al. (2016) and Vázquez-Méndez et al. (2019), the following functional J_T should be minimized:

$$J_T = \int_0^T \left(\sum_{y \in \mathcal{I}^{in}} \epsilon_y^q q_y(t) + \sum_{i=1}^{N_R} \epsilon_i \int_0^{L_i} \rho_i(s,t)\, ds - \sum_{z \in \mathcal{I}^{out}} \epsilon_z^{out} f_z(\rho_z(L_z,t)) \right) dt, \tag{5}$$

where ϵ_y^q, ϵ_i, $\epsilon_z^{out} \geq 0$ are weight parameters to be chosen by the decision makers according to their social/political preferences.

Regarding air pollution, it is essential to keep the mean concentration of NO_x as low as possible, i.e., we are involved in minimizing the cost functional J_P giving the mean pollution concentration:

$$J_P = \frac{1}{T\,|\Omega|}\int_0^T \int_\Omega \phi(x,t)\,dx\,dt, \tag{6}$$

where $|\Omega|$ denotes the usual Euclidean measure of set Ω. (We must remark here that the averaged value could be taken in any sensitive region $D \subset \Omega$ and in any time subinterval of $[0,T]$ but, for the sake of simplicity, we have chosen here the full domains).

For the *controls* (that is, the design variables that can be managed within the network), several different choices have been investigated in previous studies: incoming fluxes (Goatin et al. (2016)), drivers' preferences (Gugat et al. (2005)), network expansions (Alvarez-Vázquez et al. (2018)), etc. However, we will center our attention at the optimal management of the network intersections, attempting to obtain those α_{lk}^j, β_{kl}^j that are the most satisfactory for our global aims.

Supposing that the parameters α_{lk}^j (drivers' preferences) change when the input/output ratios β_{kl}^j are modified at the intersections, we will assume that the set of drivers always try to minimize the functional J_T, while the leader organization managing the whole network intends to choose the ratios to try to minimize atmospheric contamination.

Following this reasoning, we face up to a bilevel problem. In the lower level, we have the *follower problem*: for a given $\boldsymbol{\beta} = (\beta_{kl}^j),\ j = 1,\dots,N_J,\ k \in \mathcal{I}_j^{in},\ l \in \mathcal{I}_j^{out}$, verifying (3), solve:

$$\begin{array}{l} \min J_T(\boldsymbol{\alpha},\boldsymbol{\beta}) \\ \text{subject to (2)} \end{array} \tag{7}$$

with $\boldsymbol{\alpha} = (\alpha_{lk}^j),\ j = 1,\dots,N_J,\ k \in \mathcal{I}_j^{in},\ l \in \mathcal{I}_j^{out}$.

Then, in the upper level, the *leader problem* reads as:

$$\begin{array}{l} \min J_P(\boldsymbol{\alpha}_{\boldsymbol{\beta}},\boldsymbol{\beta}) \\ \text{subject to (3)} \end{array} \tag{8}$$

where $\boldsymbol{\alpha}_{\boldsymbol{\beta}}$ is the optimal solution of the follower problem (7) for given data $\boldsymbol{\beta}$.

In this approach, our main objective relies in computing a Stackelberg strategy for the bilevel problem (7)-(8), in the sense of below classical definition:

Definition 1 A pair $(\boldsymbol{\alpha}^*,\boldsymbol{\beta}^*)$ is said to be a Stackelberg strategy, solution of the bilevel problem (7)-(8), if it verifies that:

1. $\boldsymbol{\alpha}^*$ is the best reaction of the follower to the leader choice $\boldsymbol{\beta}^*$, i.e., $\boldsymbol{\alpha}^*$ is the solution of the follower problem (7) for given data $\boldsymbol{\beta}^*$ (in other words, $\boldsymbol{\alpha}^* = \boldsymbol{\alpha}_{\boldsymbol{\beta}^*}$).
2. $\boldsymbol{\beta}^*$ is the best option of the leader, i.e., $\boldsymbol{\beta}^*$ is the optimal solution of the leader problem (8).

We must remark here that, by using adjoint techniques (Marchuk (1986)), the functional $J_P(\boldsymbol{\alpha}, \boldsymbol{\beta})$ can be rewritten in the more useful alternative form (see full details in Theorem 3.1 of Alvarez-Vázquez et al. (2018):

$$\begin{aligned} J_P = & \sum_{i=1}^{N_R} \int_0^T \int_0^{L_i} \left(\gamma_i f_i(\rho_i(s,t)) + \eta_i \rho_i(s,t)\right) g(\sigma_i(s),t)\, ds\, dt \\ & + \sum_{y \in \mathcal{I}^{in}} \int_0^T \lambda_y q_y(t)\, g(\sigma_y(0),t)\, \chi_{S^-}(\sigma_y(0),t)\, dt + \int_\Omega \phi^0(x)\, g(x,0)\, dx, \end{aligned} \tag{9}$$

where χ_{S^-} is the characteristic function of the inflow boundary S^-, $\gamma_i f_i(\rho_i(s,t)) + \eta_i \rho_i(s,t)$ represents the pollutant emissions on the road network, and $g(\sigma_i(s),t)$ is the evaluation on the road network of the so-called *adjoint state* $g(x,t)$, the solution of the following final/boundary value problem:

$$-\frac{\partial g}{\partial t} - \mathbf{v} \cdot \nabla g - \nabla \cdot (\mu \nabla g) + \kappa g = \frac{1}{T\,|\Omega|} \quad \text{in } \Omega \times (0,T), \tag{10a}$$

$$g(x,T) = 0 \quad \text{in } \Omega, \tag{10b}$$

$$\mu \frac{\partial g}{\partial n} = 0 \quad \text{on } S^-, \tag{10c}$$

$$\mu \frac{\partial g}{\partial n} + g\mathbf{v} \cdot \mathbf{n} = 0 \quad \text{on } S^+. \tag{10d}$$

This alternative reformulation of functional (9) depends straightforwardly on traffic density and flow rate and, consequently, on the controls $(\boldsymbol{\alpha}, \boldsymbol{\beta})$. However, this control dependency is implicit (as can be seen in conditions (1c)-(1d)) making hard to get an explicit expression of the derivative of the functionals (5) and (9) with respect to the controls. This fact will be a decisive issue in the choice of methods for solving the bilevel optimal control problem.

Finally, it is important emphasizing here that the adjoint state $g(x,t)$ is the unique solution of the adjoint equation (Alvarez-Vázquez et al. (2018); Ladyzenskaja et al. (1969)), being independent of the traffic variable $\rho(x,t)$. Consequently, the adjoint state does not depend on the traffic model. So, it can be computed separately, and the adjoint problem (10) only needs to be solved once in a preliminary step.

4 Numerical solution of the bilevel optimal control problem

The bilevel problem (7)-(8) is generally non-convex. Therefore, many local solutions are expected. Moreover, effective expressions for the gradients of objective functionals J_T and J_P with respect to the controls $(\boldsymbol{\alpha}, \boldsymbol{\beta})$ are hard to compute (leading to the only reasonable option involving its numerical approximation). So, free-derivative optimization methods or methods using a numerical approximation of gradients will be the natural and efficient choice to solve the bilevel problem.

4.1 Discretization of cost functionals J_T and J_P

With independence on the method chosen to solve the bilevel problem, its efficiency relies on a good discretization and evaluation of the cost functionals J_T and J_P. So, as a previous step, we show how this can be performed in a suitable way (following the method already introduced in Vázquez-Méndez et al. 2019).

We choose the following space-time discretization: For each road A_i, the parametrization interval $I_i = [0, L_i]$ is split into M_i cells $I_{i,h} = [s_{i,h-\frac{1}{2}}, s_{i,h+\frac{1}{2}}]$, $h = 1, \ldots, M_i$, of length $\Delta s_i > 0$, where $s_{i,h} = (s_{i,h-\frac{1}{2}} + s_{i,h+\frac{1}{2}})/2$ represents the midpoint of each cell. On the other part, the time interval $[0, T]$ is also split into $N \in \mathbb{N}$ subintervals of length $\Delta t = T/N$, defining in this way the discrete times $t^n = n\Delta t,\ n = 0, \ldots, N$, are defined. Using this discretization the system (1) can be solved addressing the functional J_T with quadrature rules (Alvarez-Vázquez et al. (2015); Alvarez-Vázquez et al. (2017)). In particular, given the discrete density $\rho^n_{i,h}$ and queue q^n_i, for $n = 0, \ldots, N,\ i = 1, \ldots, N_R,\ h = 1, \ldots, M_i$, we evaluate the following full-discrete integral:

$$J_T^{\Delta} = \Delta t \sum_{n=0}^{N} \left(\sum_{y \in \mathcal{I}^{in}} \epsilon^q_y q^n_y + \sum_{i=1}^{N_R} \epsilon_i \Delta s_i \sum_{h=1}^{M_i} \rho^n_{i,h} - \sum_{z \in \mathcal{I}^{out}} \epsilon^{out}_z f_z(\rho^n_{z,M_z}) \right). \quad (11)$$

On the other part, let us consider a polygonal approximation Ω_h of Ω, with an admissible triangulation τ_h, where vertices $\{x_j,\ j = 1, \ldots, N_v\}$ satisfy that all the vertices on the boundary $\partial\Omega_h$ remain on the boundary $\partial\Omega$, that is $\sigma_y(0),\ \sigma_z(L_z) \in \partial\Omega_h$, for all $y \in \mathcal{I}^{in}$, $z \in \mathcal{I}^{out}$, and that, for $n = 0, \ldots, N-1$, each edge of $\partial\Omega_h$ lies either in $(S^n_h)^- = \{x \in \partial\Omega_h \ : \ \mathbf{v} \cdot \mathbf{n} < 0\}$ or in $(S^n_h)^+ = \{x \in \partial\Omega_h \ : \ \mathbf{v} \cdot \mathbf{n} \geq 0\}$.
Then, the adjoint model can be solved numerically on the domain Ω_h, and for the discrete times $\{t^n\}_{n=0}^N$ we get the discrete adjoint values $\{\{g^n_{h,k}\}_{k=0}^{n_v}\}_{n=0}^N$ (see Alvarez-Vázquez et al. (2015) and Algorithm 3 of Vázquez-Méndez et al. (2019)). Once this is done, it is possible to evaluate the adjoint state at roads' nodes getting $\{g^n_h(\sigma_i(s_{i,h}))\}_{i=1}^{N_R}$ by triangular interpolation. Thus, the leader functional J_P can be now addressed by quadrature rules: Given the discrete functions $\rho^n_{i,h},\ f_i(\rho^n_{i,h}),\ g^n_{h,k}$ and $g^n_h(\sigma_i(s_{i,h}))$, for $n = 1, \ldots, N,\ i = 1, \ldots, N_R,\ h = 1, \ldots, M_i$, we evaluate the following full-discrete integral:

$$\begin{aligned} J_P^{\Delta} = \Delta t \sum_{n=1}^{N} \sum_{i=1}^{N_R} \sum_{h=1}^{M_i} \Delta s_i (\gamma_i f_i(\rho^n_{i,h}) + \eta_i \rho^n_{i,h}) g^n_h(\sigma_i(s_{i,h})) \|\sigma_i'(s_{i,h})\| \\ + \sum_{n=1}^{N} \sum_{\substack{y \in \mathcal{I}^{in} \\ \sigma_y(0) \in (S^n_h)^-}} \lambda_y q^n_y g^n_h(\sigma_y(s_{y,1})) + \frac{1}{3} \sum_{\mathcal{T} \in \tau_h} |\mathcal{T}| \sum_{x_j \in \mathcal{T}} \Phi^0(x_j) g^0_j \end{aligned} \quad (12)$$

It is worthwhile remarking here that each evaluation of the discrete functionals J_T^{Δ} and J_P^{Δ} for a pair $(\boldsymbol{\alpha}, \boldsymbol{\beta})$ requires the solution of the LWR traffic model

(1), the computation of the adjoint state, and also evaluate the objective functionals. All those computations requires efficient algorithms, see for instance Algorithms 1,2,3 and 4 of Vázquez-Méndez et al. (2019).

4.2 Solving the follower problem

Given the discrete cost functional J_T^{Δ}, the follower problem (7) will be solved by combining an interior-point method and a genetic algorithm. Both algorithms are implemented respectively by the solvers `fmincon` and `ga` from the Optimization Toolbox of Matlab R2017a, being important the following issues: The solver `ga` includes a `hybrid` option that allows combining it with other Matlab optimization solvers, can be executed in parallel, and uses the three basic *probabilistic rules* of the natural selection: elite, crossover and mutation to generate the next generation (cf. Algorithm 1). On the other part, the solver `fmincon` can approximate the cost functional gradient in case of not availability (like our case) and can be also executed in parallel. Moreover, the direction-search of solver `ga` presents a large set of probabilities provided by the population diversity; in contrast, in the solver `fmincon` the direction-search is given by a line-search and trust-region criterion which depends on the direct-step or conjugate-gradient step. Then, to provide `fmincon` with a diversity similar to `ga`, in this work a multi-start execution of `fmincon` was carried out (see full details in Algorithm 2).

Algorithm 1: `ga` algorithm with hybrid option

Data: Initial arrays population $\tilde{\boldsymbol{\alpha}}^0 = \{\boldsymbol{\alpha}^{0,n}\}_{n=1}^N$, fixed array $\boldsymbol{\beta}$, and tolerance *tol*
Result: Optimal array of preferences $\boldsymbol{\alpha}^*$, and optimal functional value $J_T^{\Delta}(\boldsymbol{\alpha}^*, \boldsymbol{\beta})$
begin
  `set` $k = 0$;
  while $Error > tol$ **do**
    for $n = 1, ..., N$ **do**
      `Compute` $J_T^{\Delta}(\boldsymbol{\alpha}^{k,n}, \boldsymbol{\beta})$ by `Algorithm 2` of Vázquez-Méndez et al. (2019)
    end
    `Generate` the new population $\tilde{\alpha}^{k+1}$ by natural selection: `Elite, Crossover` and `Mutation`;
    `Compute` *Error* and `set` $k = k + 1$;
  end
  `set` $\bar{\boldsymbol{\alpha}}$ as the array corresponding to the minimum of the functional value set $\{J_T(\boldsymbol{\alpha}^{k+1,n}, \boldsymbol{\beta})\}_{n=1}^N$;
  `switch` to `fmincon`;
  `input` $\bar{\boldsymbol{\alpha}}$ and `compute` min $J_T^{\Delta}(\boldsymbol{\alpha}, \boldsymbol{\beta})$ by `fmincon`, and `get` the optimal $\boldsymbol{\alpha}^*$ and the optimal functional value $J_T^{\Delta}(\boldsymbol{\alpha}^*, \boldsymbol{\beta})$;
end

Algorithm 2: `fmincon multi-start` algorithm

Data: Multi-initial arrays set $\boldsymbol{\alpha} = \{\boldsymbol{\alpha}_0^i\}_{i=1}^N$, fixed array $\boldsymbol{\beta}$, and tolerance *tol*
Result: Optimal array of preferences $\boldsymbol{\alpha}^*$, and optimal functional value $J_T^{\Delta}(\boldsymbol{\alpha}^*, \boldsymbol{\beta})$
begin
  for $i = 1, ..., N$ **do**
    `Input` $\boldsymbol{\alpha}_0^i$ and `compute` $\min J_T^{\Delta}(\boldsymbol{\alpha}, \boldsymbol{\beta})$ by `fmincon` and get the optimal $\boldsymbol{\alpha}^{*,i}$
  end
  `set` $J_T^{\Delta}(\boldsymbol{\alpha}^*, \boldsymbol{\beta}) = \min\{J_T^{\Delta}(\boldsymbol{\alpha}^i, \boldsymbol{\beta})\}_i^N$;
  `set` $\boldsymbol{\alpha}^*$ as the best from $\{\boldsymbol{\alpha}^{*,i}\}_{i=1}^N$;
end

4.3 Solving the leader problem

To compute the Stackelberg solution $(\boldsymbol{\alpha}^*, \boldsymbol{\beta}^*)$ in the sense of Definition 1, a combination between the solvers `ga-hybrid` (Algorithm 1) and `fmincon` multi-start (Algorithm 2) will be used, with the aim of addressing the complexity of the leader problem. Thus, the diversity at searching directions provided by `ga` could be used for identifying a feasible initial value for the `fmincon`, getting in this way a high-quality Stackelberg solution. Nevertheless, since this hybrid method only gives $\boldsymbol{\beta}^*$ as output, the best follower response $\boldsymbol{\alpha}^*$ to the leader is computed and saved from the last leader's functional evaluation in the convergent sequence $\boldsymbol{\beta}_k \to \boldsymbol{\beta}^*$ at the `fmincon` stage of the hybrid solver. The details of this process are shown in Algorithm 3, where the use of the adjoint state provides an important saving in the total computational cost.

5 Numerical experiences

Although we have carried out numerous numerical experiments, we only present and analyse here, for the sake of brevity, some computational results obtained in a real-world scenario in Mexico, set in the Guadalajara Metropolitan Area (GMA). Given the previous experiences over the same domain developed by the authors in Alvarez-Vázquez et al. (2017); Alvarez-Vázquez et al. (2018); Vázquez-Méndez et al. (2019) we only recall here essential data and assumptions in a summarized way.

5.1 Initial/boundary conditions and models parameters

The road network analyzed here is composed by $N_R = 17$ avenues and $N_J = 9$ junctions, where all avenues have only one lane and its theoretical flow is regulated by the static relation defined in Alvarez-Vázquez et al. (2018). As boundary conditions for the traffic model (1), we consider equal downstream road capacities for the 3 incoming avenues ($C_i^{in} = 2.013\,10^3,\ i = 1, 2, 10$), with equal sinusoidal desired inflow rate, and also equal maximum outflow rates for the 3 outgoing roads ($f_z^k = 2.013\,10^3,\ k = 13, 14, 15$). As initial conditions,

Algorithm 3: Stackelberg algorithm

Data: Initial arrays population $\tilde{\boldsymbol{\beta}}^0 = \{\boldsymbol{\beta}^{0,n}\}_{n=1}^N$
Result: Stackelberg solution $(\boldsymbol{\alpha}^*, \boldsymbol{\beta}^*)$, and optimal functional values $J_T^{\Delta}(\boldsymbol{\alpha}^*, \boldsymbol{\beta}^*), J_P^{\Delta}(\boldsymbol{\alpha}^*, \boldsymbol{\beta}^*)$
begin
  `set` $k = 0$ and `compute` the adjoint $g_{h,k}^n$ by `Algorithm 3` of Vázquez-Méndez et al. (2019);
  while $Error > tol$ **do**
    for $n = 1, ..., N$ **do**
      `set` randomly $\boldsymbol{\alpha} = \{\boldsymbol{\alpha}_0^i\}_{i=1}^M$ as multi-initial arrays set;
      `Input` $\boldsymbol{\alpha}$ and `compute` min $J_T^{\Delta}(\boldsymbol{\alpha}, \boldsymbol{\beta}^{k,n})$ by `Algorithm 2`, and get $\boldsymbol{\alpha}_{\boldsymbol{\beta}^{k,n}}$;
      `Compute` $J_P^{\Delta}(\boldsymbol{\alpha}_{\boldsymbol{\beta}^{k,n}}, \boldsymbol{\beta}^{k,n})$ by `Algorithm 4` of Vázquez-Méndez et al. (2019) ;
    end
    `Generate` the next population $\tilde{\beta}^{k+1}$ by natural selection: `Elite, Crossover and Mutation`;
    `Compute` $Error$ and `set` $k = k + 1$;
  end
  `set` $\bar{\boldsymbol{\beta}}$ as the array corresponding to the minimum from the functional values set $\{J_P(\boldsymbol{\alpha}, \boldsymbol{\beta}^{k+1,n})\}_{n=1}^N$;
  `switch` to `fmincon`;
  `input` $\bar{\boldsymbol{\beta}}$ and `compute` min $J_P^{\Delta}(\boldsymbol{\alpha}, \boldsymbol{\beta})$ by `fmincon`, and `get` $\boldsymbol{\beta}^*$;
  from the last evaluation of $J_P^{\Delta}(\boldsymbol{\alpha}, \boldsymbol{\beta})$ `get` $\boldsymbol{\alpha}^*$;
  `Compute` $J_T^{\Delta}(\boldsymbol{\alpha}^*, \boldsymbol{\beta}^*)$ and $J_P^{\Delta}(\boldsymbol{\alpha}^*, \boldsymbol{\beta}^*)$
end

null traffic ($\rho_{i,s}^0 = 0,\ i = 1, ..., N_R$) and queues ($q_y^0 = 0,\ y = 1, 2, 10$) were assumed. Also, we have considered the following weights parameters: For the road densities $\epsilon_i = 0.7,\ i = 1, 2, 3$ and $\epsilon_i = 0.5$ for the rest of avenues, for queue lengths $\epsilon_i^q = 0.45,\ i = 1, 2$ and $\epsilon_{10}^q = 0.1$, and for outflow rates $\epsilon_z^{out} = 0.5,\ z = 13, 14, 15$. This combination of weights values translates the intention of increasing the follower cost by an excess of traffic densities and/or queue lengths.

With respect to the pollution model (4) and its corresponding adjoint state (10), typical values for NO_x ($\mu = 3.5\,10^{-8}\,\mathrm{km}^2/\mathrm{h}, \kappa = 0.610^{-2}\mathrm{h}^{-1}, \gamma_i = 10^6\,\mathrm{kg}/$ number of cars/km, $\eta_i = 3.1610^{-5}$ kg/number of cars/h) have been taken. We also consider null pollution at initial time, not external pollution sources and, due to the particular wind direction at S^+ (see Fig. 3), parameters $\lambda_y = 0$.

Regarding the discretization, we chose a time step of $\Delta t = 4\,10^{-3}$ (measured in hours) and, for each road A_i, its spatial domain I_i has been divided into cells large enough to guarantee the classical CFL condition ($\Delta s_i \in (0.2, 0.21)$). Finally the polygonal domain $\Omega_h \subset \mathbb{R}^2$ has been discretized with a triangulation of 898 triangles and 491 vertices, satisfying standard regularity hypothesis, to guarantee the numerical method convergence (Geuzaine and Remacle (2009)). It is important to remark here that we have developed many examples with different discretization strategies and different resolutions of

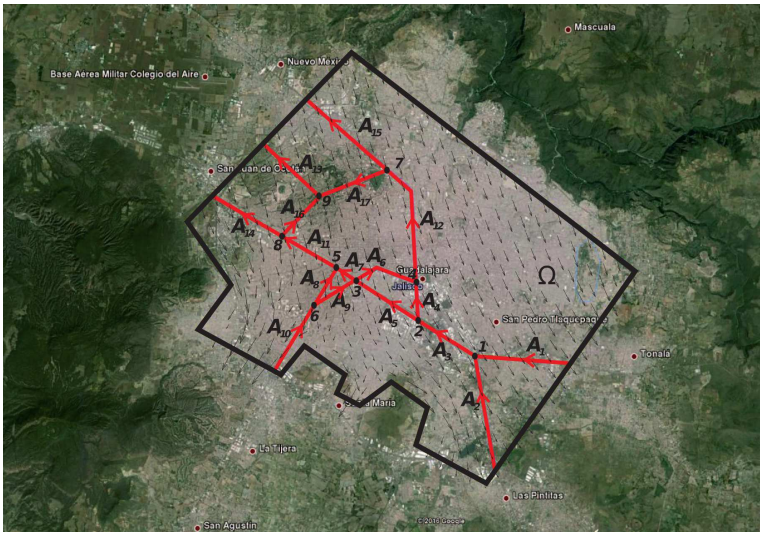

Fig. 3 Satellite photo of the GMA: The polygonal domain Ω_h and the vectors represent the wind field are drawn in black, the road network in red

time steps (finer or coarser), and the final results have been always qualitatively similar. So, it seems that these choices do not affect the achieved optimal solutions.

With respect to the minimization algorithms, we consider an initial population of 50 individuals for the `ga` and `ga-hybrid` solvers, and a set of 5 arrays as initial input for the `fmincon-multi-start` solver. All solvers have been executed in parallel in an AMD Threadripped 1920X CPU at 3.8 GHz with 12 cores and 24 threads desktop, 32 GB RAM, and Linux Mint OS.

5.2 Assessment experiences for solving the follower problem

In the follower problem (7) the restrictions array $\boldsymbol{\beta} = \{\beta_{kl}^{j}\}$ must be fixed and, in this particular experience, it will be chosen in such a manner that we can predict the preferences array $\boldsymbol{\alpha} = \{\alpha_{lk}^{j}\}$ and, consequently, can confirm the reliability of our approach. Then, in this spirit, two different representative cases are shown.

Case 1: In this first case, the restrictions $\beta_{kl}^{1,j}$ are taken such that the avenues A_5, A_6 and A_7 remain blocked at intersections $j = 3, 4$ and 5 (that is, $\beta_{5\,6}^{1,3} = \beta_{5\,7}^{1,3} = \beta_{6\,12}^{1,4} = \beta_{7\,11}^{1,5} = 0$). Then, it is expected that the drivers coming from A_3 and A_{10} take the avenues A_4 and A_8, respectively, avoiding the block imposed by the leader. In this case it is also expected that drivers take their respective outways by avenues A_{12} and A_{11}. Thus, arrays $\beta_{kl}^{1,j}$ were fixed satisfying above constraints (see Table 1) and then the follower problem was solved

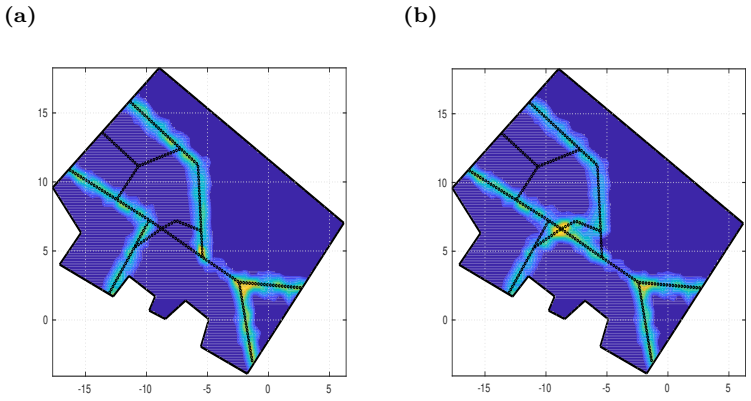

Fig. 4 Level curves of the mean concentrations of pollution for a simulation period of 24 hours with zero wind **a** Case 1 and **b** Case 2

using `ga-hybrid`, `ga` and `fmincon-multi-start` routines. These solvers were addressed with a tolerance of 10^{-4} (although in the hybrid case an additional tolerance of 10^{-10} was imposed), and the corresponding resulting preferences, respectively denoted by $\alpha_{lk}^{hyb,j}, \alpha_{lk}^{ga,j}$ and $\alpha_{lk}^{fmin,j}$, are shown in Table 1.

Here, the three solutions present in common the preferences $\alpha_{4\,3}^{2} = 1, \alpha_{8\,10}^{6} = 1$, which imply that all drivers from A_3 and A_{10} take the avenues A_4 and A_8 at junctions $j = 2$ and $j = 6$, avoiding the blocked avenues A_5, A_6 and A_7. To confirm this, in Figure 4a the isolines of pollution concentration (with zero wind $\mathbf{v} = 0$) are depicted, showing in a clear way in which avenues the pollutant emissions are present (and consequently the traffic flow is high). Therefore, the predicted behavior of drivers is fulfilled for this first case.

Case 2: For this second case we have chosen $\beta_{kl}^{2,j}$ such that we block the avenues A_4 and A_8 at intersections $j = 4, 5$ (that is, $\beta_{4\,12}^{2,4} = \beta_{8\,11}^{2,5} = 0$), and we let free pass of vehicles from A_5 to A_7 and also from A_9 to A_6 (that is, $\beta_{9\,6}^{2,3} = \beta_{5\,7}^{2,3} = 1$). Then, it is expected that drivers from A_3 and A_{10} will turn on $A_5 - A_7$ and $A_9 - A_6$, respectively, avoiding the blocked avenues A_8 and A_4. Also for this case, drivers should take their outways at avenues A_{12} and A_{11}, respectively. So, once fixed the arrays $\beta_{kl}^{2,j}$ in this manner (see full details in Table 1), the follower problem was addressed again by using solvers `ga-hybrid`, `ga` and `fmincon-multi-start`. The corresponding preferences resulting from these solvers, denoted by $\alpha_{lk}^{hyb,j}, \alpha_{lk}^{ga,j}$ and $\alpha_{lk}^{fmin,j}$, can be also found in Table 1.

In this case, the three solutions are equal in practice, and the key of this fact relies on the achieved matrices of preferences at junction $j = 3$. In these matrices, the values of preferences indicate that all drivers from A_5 prefer taking A_7 ($\alpha_{7\,5}^{3} = 1$) and all drivers from A_9 prefer taking A_6 ($\alpha_{6\,9}^{3} = 1$), avoiding in this way the blocked avenues A_4 and A_8. This could be checked in

Table 1 Data for the two analyzed cases of the follower problem (7): The fixed leader restrictions $\beta_{kl}^{1,j}$ and $\beta_{kl}^{2,j}$ correspond to Case 1 and Case 2, respectively. For each case, the optimal preferences $\alpha_{lk}^{solver,j}$ for the three solvers (`fmincon, hybrid, ga`) are also displayed.

	j=1	j=2	j=3	j=4	j=5	j=6	j=7	j=8	j=9
$\mathcal{I}_j^{in}(k)$	$\{1,2\}$	$\{3\}$	$\{5,9\}$	$\{4,6\}$	$\{7,8\}$	$\{10\}$	$\{12\}$	$\{11\}$	$\{16,17\}$
$\mathcal{I}_j^{out}(l)$	$\{3\}$	$\{4,5\}$	$\{6,7\}$	$\{12\}$	$\{11\}$	$\{8,9\}$	$\{15,17\}$	$\{14,16\}$	$\{13\}$
$\beta_{kl}^{1,j}$	$\begin{bmatrix}0.5\\0.5\end{bmatrix}$	$(1,1)$	$\begin{bmatrix}0.00 & 0.00\\1.00 & 1.00\end{bmatrix}$	$\begin{bmatrix}1.00\\0.00\end{bmatrix}$	$\begin{bmatrix}0.00\\1.00\end{bmatrix}$	$(1,1)$	$(1,1)$	$(1,1)$	$\begin{bmatrix}0.5\\0.5\end{bmatrix}$
$\alpha_{lk}^{hyb,j}$	$(1,1)$	$\begin{bmatrix}1.00\\0.00\end{bmatrix}$	$\begin{bmatrix}0.40 & 0.16\\0.60 & 0.84\end{bmatrix}$	$(1,1)$	$(1,1)$	$\begin{bmatrix}1.00\\0.00\end{bmatrix}$	$\begin{bmatrix}1.00\\0.00\end{bmatrix}$	$\begin{bmatrix}1.00\\0.00\end{bmatrix}$	$(1,1)$
$\alpha_{lk}^{ga,j}$	$(1,1)$	$\begin{bmatrix}1.00\\0.00\end{bmatrix}$	$\begin{bmatrix}0.38 & 0.02\\0.62 & 0.98\end{bmatrix}$	$(1,1)$	$(1,1)$	$\begin{bmatrix}1.00\\0.00\end{bmatrix}$	$\begin{bmatrix}1.00\\0.00\end{bmatrix}$	$\begin{bmatrix}1.00\\0.00\end{bmatrix}$	$(1,1)$
$\alpha_{lk}^{fmin,j}$	$(1,1)$	$\begin{bmatrix}0.99\\0.01\end{bmatrix}$	$\begin{bmatrix}0.73 & 0.71\\0.27 & 0.29\end{bmatrix}$	$(1,1)$	$(1,1)$	$\begin{bmatrix}1.00\\0.00\end{bmatrix}$	$\begin{bmatrix}1.00\\0.00\end{bmatrix}$	$\begin{bmatrix}1.00\\0.00\end{bmatrix}$	$(1,1)$
$\beta_{k,l}^{2,j}$	$\begin{bmatrix}0.5\\0.5\end{bmatrix}$	$(1,1)$	$\begin{bmatrix}0.00 & 1.00\\1.00 & 0.00\end{bmatrix}$	$\begin{bmatrix}0.00\\1.00\end{bmatrix}$	$\begin{bmatrix}1.00\\0.00\end{bmatrix}$	$(1,1)$	$(1,1)$	$(1,1)$	$\begin{bmatrix}0.5\\0.5\end{bmatrix}$
$\alpha_{lk}^{hyb,j}$	$(1,1)$	$\begin{bmatrix}0.00\\1.00\end{bmatrix}$	$\begin{bmatrix}0.00 & 1.00\\1.00 & 0.00\end{bmatrix}$	$(1,1)$	$(1,1)$	$\begin{bmatrix}0.00\\1.00\end{bmatrix}$	$\begin{bmatrix}1.00\\0.00\end{bmatrix}$	$\begin{bmatrix}1.00\\0.00\end{bmatrix}$	$(1,1)$
$\alpha_{lk}^{ga,j}$	$(1,1)$	$\begin{bmatrix}0.00\\1.00\end{bmatrix}$	$\begin{bmatrix}0.00 & 1.00\\1.00 & 0.0\end{bmatrix}$	$(1,1)$	$(1,1)$	$\begin{bmatrix}0.00\\1.00\end{bmatrix}$	$\begin{bmatrix}1.00\\0.00\end{bmatrix}$	$\begin{bmatrix}1.00\\0.00\end{bmatrix}$	$(1,1)$
$\alpha_{lk}^{fmin,j}$	$(1,1)$	$\begin{bmatrix}0.00\\1.00\end{bmatrix}$	$\begin{bmatrix}0.00 & 1.00\\1.00 & 0.00\end{bmatrix}$	$(1,1)$	$(1,1)$	$\begin{bmatrix}0.00\\1.00\end{bmatrix}$	$\begin{bmatrix}1.00\\0.00\end{bmatrix}$	$\begin{bmatrix}1.00\\0.00\end{bmatrix}$	$(1,1)$

Table 2 Computational data of the different solvers for Case 2.

Solver	$J_T^{\Delta}(\alpha^{opt},\beta^2)$	iterations	evaluations	time (min)
`ga-hybrid`	$1.1300\,10^4$	98	4955	57.93
`ga`	$1.1312\,10^4$	94	4750	47.84
`fmincon`	$1.1349\,10^4$	10	75	17.48

the level curves of pollution shown in Figure 4b. As in the previous case, the predicted behavior of drivers is also fulfilled for this new case. It is interesting commenting here that in both cases (and in other instances developed by the authors but not shown here) drivers did not take roads A_{13}, A_{16} or A_{17} unless they were forced to do it. This fact may mean that, in practice, transportation authorities could consider the option of removing them from the network without any dramatic consequence for traffic.

Finally, the effectiveness and the computational cost (accuracy of the solution, number of cost functional evaluations and computation time) of the three options to solve the follower problem were evaluated, but for the sake of conciseness, only the output from Case 2 is shown. So, in Table 2 the discrete cost function J_T^{Δ} evaluated in the optimal solution, the number of functional evaluations and the solver execution time is shown. As can be seen there, the hybrid method and the genetic algorithm present better effectiveness but at a much higher computational cost and execution time; in contrast, the `fmincon` solver has slightly poorer effectiveness but with a significantly lower compu-

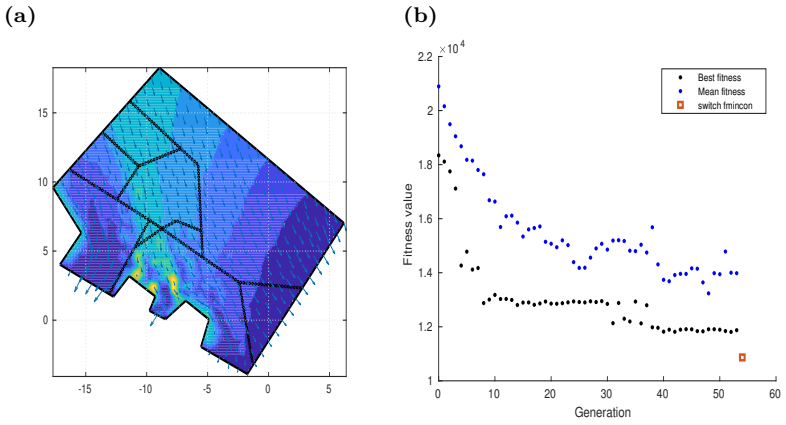

Fig. 5 Level curves of the time-averaged adjoint discretized state employed for the optimization process **a**, evolution of the number of iterations for the solver `ga-hybrid`, including the `fmincon` solution **b**

tational cost, being consistent with the smallest dimension of its initial arrays set.

5.3 A highly restrictive Stackelberg solution

As commented in the above sections, as a previous step in the evaluation of J_P^A, the adjoint model needs to be solved (only once). The isolines of the discretized adjoint state (averaged for a time interval of 24 hours) are shown in Fig. 5a, with minimum values near the outflow boundary S^- (except in a few small zones), and it increases as we get closer to the inflow boundary S^+. This tendency indicates that to reduce the leader functional (which includes the product of the adjoint evaluated on roads and their corresponding emissions), the traffic must be concentrated in the roads located in the low zone of the domain. Therefore, it is expected that the leader's effort (using the restrictions on network intersections) should be directed to block the access of drivers to the top part of the domain.

The Stackelberg solution $(\boldsymbol{\alpha}^*, \boldsymbol{\beta}^*)$ is displayed in Table 3, and an analysis of the computational effort of the optimization process can be found in Fig. 5b. In this Stackelberg solution, restrictions $\beta^{*,3}_{5\,6} = \beta^{*,3}_{5\,7} = \beta^{*,4}_{4\,12} = 0$ indicate that the leader blocks the avenue A_5 at junction $j = 3$, and avenue A_4 at junction $j = 4$; on the contrary, $\beta^{*,5}_{8\,11} = 1$ leaves free pass to cars from A_8 at junction $j = 5$. With this strategy, the leader leaves to the follower with only an outway at $A_{11} - A_{14}$ avenues for those vehicles that enter by A_{10}, meanwhile vehicles that enter by A_1 and A_2 remains blocked in avenues A_1, A_2, A_3, A_4. This allows the leader to reach the objective of prevent drivers to take A_6, A_{12} and A_{15} which conduce to the upper part of the domain. With these blocked avenues the follower takes the (only) outway left for the leader ($\alpha^{*,6}_{8\,10} = 1$) and

prefers the blocked A_4 instead of the blocked A_5 ($\alpha^{*,2}_{4\,3} = 1$). As a consequence of this preferences and restrictions, $(\boldsymbol{\alpha}^*, \boldsymbol{\beta}^*)$ are bottlenecks at intersections $j = 1, 2, 4$, with large queue lengths at A_1, A_2 that maximize the length queue mean (Fig. 7c), with low presence of vehicles in upper domain avenues (Fig. 6c), but with a large mean density (Fig. 7a), and low outflow at exit-points of the road network (Fig. 7d). Therefore, a lower pollution levels are expected at most of the domain, and the higher levels are limited to specific zones close to the inferior boundary, as confirmed in Fig. 8c. This situation is congruent with the prediction deduced above using the solution of the adjoint model.

It is important remarking here that, in contrast, the follower solution in above Case 2 (that will be taken here as a non-optimal case), do not present any blocked avenue and all densities are below ρ_{max} in the whole network. Consequently, a better distribution of the density is reached (see Fig. 6a) giving lower density, higher flow, fewer queues and finally more outflow with respect to the Stackelberg solution, but at to expense of a more polluted city (compare Figs. 8a and 8c). All previous results suggest a worse situation for drivers in the Stackelberg solution, with large travel times to ensure low pollution levels. This is confirmed by the values displayed in Table 4, where the Stackelberg solution reduces the mean pollution by more than 112% but increases dramatically the value of the traffic-related cost functional by four times (mainly involving traffic flow and queue length).

Is clear that this Stackelberg solution is easy to explain, agrees with all the methodology exposed and fulfills the predictions made. This strongly suggests that the correct solution was obtained, but in a realistic local government situation, it is not possible to apply this (so restrictive) strategy to prevent the entry of vehicles in the city in order to reduce the urban pollution levels. So, in the following subsection, we will present a Stackelberg solution with *relaxed* restrictions.

5.4 A relaxed Stackelberg solution

In order to relax the traffic restrictions (avoiding the complete blockage of any avenue), the constraints (3) for the leader problem are changed to $0.2 \leq \beta^j_{kl} \leq 0.8$ and $\sum_{k\in\mathcal{I}^{in}_j} \beta^j_{kl} = 1$. That is, the leader lets pass between 20% and 80% of vehicles from avenue $k \in \mathcal{I}^{in}_j$ to avenue $l \in \mathcal{I}^{out}_j$ at junction j, avoiding fully blocked avenues.

The relaxed Stackelberg solution $(\boldsymbol{\alpha}^r, \boldsymbol{\beta}^r)$ is qualitatively similar to the restrictive case: It allows passing a minimum of vehicles to the upper part of the network, limits the traffic congestion to the inferior part of the city, and leaves to the follower the same outway by avenue A_{14}. This can be observed in Table 3, where the drivers' preferences $\alpha^{r,2}_{4,3} = 0, \alpha^{r,3}_{6\,5} = 0.08, \alpha^{r,3}_{6\,9} = 0.34, \alpha^{r,6}_{9\,10} = 0.06$ indicate that avenues A_4, A_6, A_{12} are not chosen by drivers, allowing the leader to impose low restrictions $\beta^{r,1}_{9\,6} = \beta^{r,4}_{6\,12} = 0.20$. Meanwhile, the restrictions $\beta^{r,1}_{1\,3} = 0.79, \beta^{r,3}_{5\,7} = \beta^{r,5}_{11\,7} = 0.80$ give pass priority to the flows

Table 3 Values of Stackelberg solutions for the bilevel problem (7)-(8): $(\boldsymbol{\alpha}^*, \boldsymbol{\beta}^*)$ stands for the highly restrictive case, and $(\boldsymbol{\alpha}^r, \boldsymbol{\beta}^r)$ for the relaxed one

	j=1	j=2	j=3	j=4	j=5	j=6	j=7	j=8	j=9
$\mathcal{I}_j^{in}(k)$	$\{1,2\}$	$\{3\}$	$\{5,9\}$	$\{4,6\}$	$\{7,8\}$	$\{10\}$	$\{12\}$	$\{11\}$	$\{16,17\}$
$\mathcal{I}_j^{out}(l)$	$\{3\}$	$\{4,5\}$	$\{6,7\}$	$\{12\}$	$\{11\}$	$\{8,9\}$	$\{15,17\}$	$\{14,16\}$	$\{13\}$
$\alpha_{lk}^{*,j}$	$(1,1)$	$\begin{bmatrix}1.00\\0.00\end{bmatrix}$	$\begin{bmatrix}0.49 & 1.00\\0.51 & 0.00\end{bmatrix}$	$(1,1)$	$(1,1)$	$\begin{bmatrix}1.00\\0.00\end{bmatrix}$	$\begin{bmatrix}1.00\\0.00\end{bmatrix}$	$\begin{bmatrix}1.00\\0.00\end{bmatrix}$	$(1,1)$
$\beta_{kl}^{*,j}$	$\begin{bmatrix}0.00\\1.00\end{bmatrix}$	$(1,1)$	$\begin{bmatrix}0.00 & 0.00\\1.00 & 1.00\end{bmatrix}$	$\begin{bmatrix}0.00\\1.00\end{bmatrix}$	$\begin{bmatrix}0.00\\1.00\end{bmatrix}$	$(1,1)$	$(1,1)$	$(1,1)$	$\begin{bmatrix}0.5\\0.5\end{bmatrix}$
$\alpha_{lk}^{r,j}$	$(1,1)$	$\begin{bmatrix}0.00\\1.00\end{bmatrix}$	$\begin{bmatrix}0.08 & 0.34\\0.92 & 0.66\end{bmatrix}$	$(1,1)$	$(1,1)$	$\begin{bmatrix}0.94\\0.06\end{bmatrix}$	$\begin{bmatrix}1.00\\0.00\end{bmatrix}$	$\begin{bmatrix}1.00\\0.00\end{bmatrix}$	$(1,1)$
$\beta_{kl}^{r,j}$	$\begin{bmatrix}0.79\\0.21\end{bmatrix}$	$(1,1)$	$\begin{bmatrix}0.79 & 0.79\\0.21 & 0.21\end{bmatrix}$	$\begin{bmatrix}0.80\\0.20\end{bmatrix}$	$\begin{bmatrix}0.80\\0.20\end{bmatrix}$	$(1,1)$	$(1,1)$	$(1,1)$	$\begin{bmatrix}0.5\\0.5\end{bmatrix}$

Table 4 Numerical values of objective functionals J_P^A and J_T^A for different strategies.

Case	$J_P^A(\boldsymbol{\alpha}, \boldsymbol{\beta})$	$J_T^A(\boldsymbol{\alpha}, \boldsymbol{\beta})$
Restrictive Stackelberg	$1.0866\,10^4$	$5.9695\,10^4$
Relaxed Stackelberg	$1.9271\,10^4$	$4.8625\,10^4$
Non-optimal (Case 2)	$2.2938\,10^4$	$1.1300\,10^4$

of vehicles in avenues $A_1, A_3, A_5, A_7, A_{11}$, limiting the traffic congestion to avenues A_2, A_8, A_9 in the inferior part of the network (see Fig. 6b and Fig.8b).

These restrictions and preferences generate the functional costs values given in Table 4, showing that this relaxed solution presents a decrease in its effectiveness (respect to the non-optimal Case 2) reducing the mean pollution in a 16%, but worsening traffic conditions (although less than in the restrictive case). These results also suggest that the pollution levels increase as the restrictions are more relaxed, making it harder for the leader to prevent traffic flows on the upper part of the network.

6 Conclusions

In this work, a bilevel optimal control problem was addressed in the sense of Stackelberg optimization. In the problem, the local government (leader) has as objective dropping down the urban pollution levels using traffic restrictions, meanwhile, the drivers (follower) have the objective of minimizing their travel-time following their preferences. The optimal solution was obtained using a combination of genetic and interior-point algorithms applied to previous numerical simulations of the traffic on an urban road network, of its pollution emissions and the pollutant transport over the whole urban domain.

To save computational efforts, adjoint techniques were used. However, the impossibility of deriving an exact gradient of the objectives with respect to the restrictions and preferences implied a large computational cost for getting a Stackelberg solution.

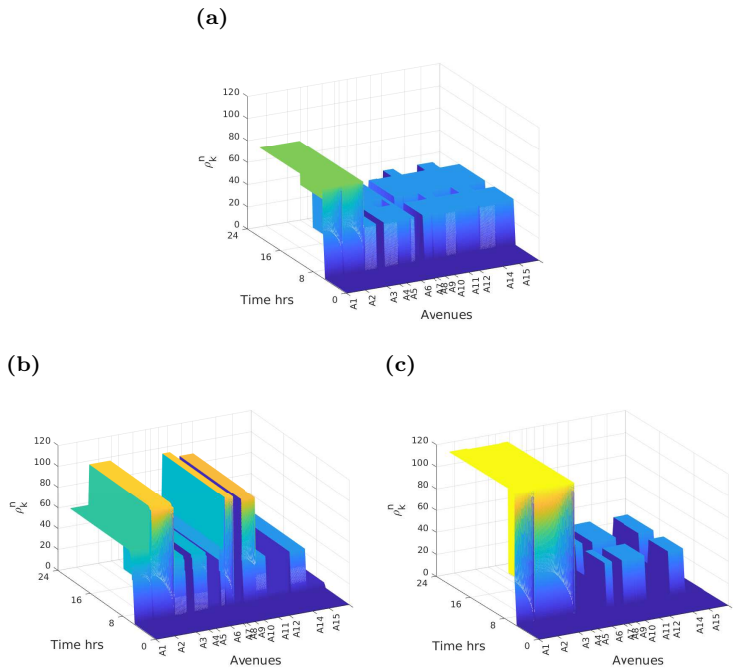

Fig. 6 Time and spatial evolution of vehicle density at selected avenues for the three cases: non-optimal **a**, relaxed Stackelberg **b** and restrictive Stackelberg **c** The Stackelberg solutions generate congestion in some avenues (ρ close to $\rho^{max} = 120$)

The numerical experiences showed that the effectiveness of the Stackelberg solution is higher when the restrictions were such that a complete blockage of traffic at road intersection is allowed, minimizing the pollution levels and increasing the travel time. This effectiveness presents a significant drop down when the restrictions are relaxed. This fact agrees, in a roughly way, with the above referenced empirical studies where data showed a progressive increase of pollution levels from non-traffic zones to traffic ones.

Finally, future research work could be related to modifications in the objectives for both, the leader and the follower. So, the queue length could be considered as an additional leader objective, removing it from the follower cost. Also, future work could consider more sophisticated improvements in the traffic model, making it more complex and realistic for urban domains. The macroscopic models with dynamic velocity and the LWR model with diffusion and different forcing (traffic-lights, multiple lanes, in-out ramps...) are options available in the specialized literature (Treiber and Kesting (2013)).

Acknowledgements First author thanks the support from Sistema Nacional de Investigadores (Mexico) under Grant SNI-52768, Programa para el Desarrollo Profesional Docente (Mexico) under Grant PRODEP/103.5/16/8066, and CONACyT by Ciencia de Frontera (Mexico) under Grant 217556. Third and fourth authors were partially supported by Xunta de Galicia under Grant ED431C 2018/50.

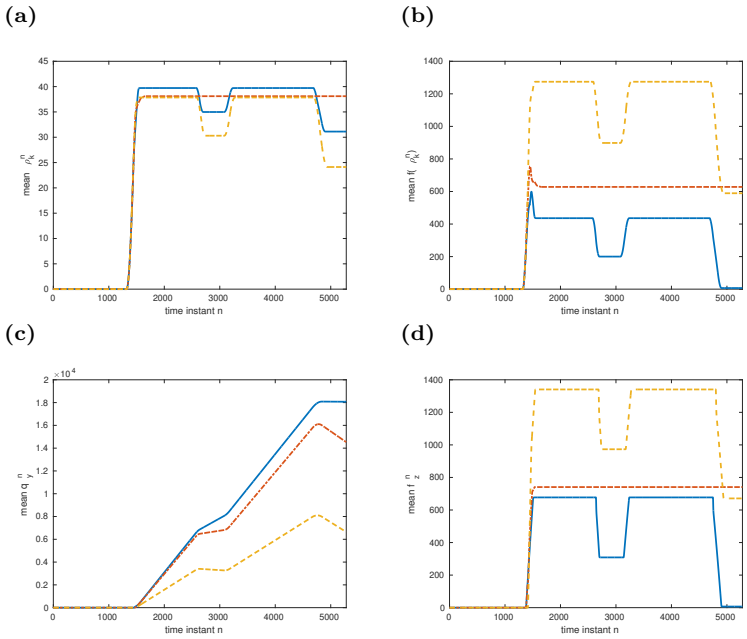

Fig. 7 Mean values of traffic variables throughout the whole network density **a**, flow **b**, queue length **c** and out flow **d** corresponding to the highly restrictive Stackelberg (solid lines), the relaxed Stackelberg (dash-point lines), and the non-optimal (dashed lines)

References

1. AbuAli, N. and Abou-zeid, H. (2016) Driver Behavior Modeling: Developments and Future Directions. Int J Veh Technol, 1-12. doi:10.1155/2016/6952791.
2. Alvarez-Vázquez LJ, García-Chan N, Martínez A, M.E. Vázquez-Méndez (2015a) An application of interactive multi-criteria optimization to air pollution control. Optimization. 64:1367–1380.
3. Alvarez-Vázquez LJ, García-Chan N, Martínez A, M.E. Vázquez-Méndez (2015b) Stackelberg strategies for wastewater management. J Comput App Math. 280:217–203.
4. Alvarez-Vázquez LJ, García-Chan N, Martínez A, M.E. Vázquez-Méndez (2017) Numerical simulation of air pollution due to traffic flow in urban networks. J Comput Appl Math. 326:44–61.
5. Alvarez-Vázquez LJ, García-Chan N, Martínez A, M.E. Vázquez-Méndez (2018) Optimal control of urban air pollution related to traffic flow in road networks. Math Control Rel Fields. 8:177–193.
6. Berrone S, de Santi F, Pieraccini S, et al (2012) Coupling traffic models on networks and urban dispersion models for simulating sustainable mobility strategies. Comput Math Appl. 64:1975–1991.
7. Bigazzia AY, Rouleau M. (2017) Can traffic management strategies improve urban air quality? A review of the evidence. J Trans Health. 7B:111–124.
8. Casas E (1997) Pontryagin's principle for state constrained boundary control problems of semilinear parabolic equations. SIAM J Control Optim. 35:1297–1327.
9. Canic S, Piccoli B, Qiu J, et al (2015) Runge-Kutta discontinuos Galerkin method for traffic flux model on networks. J Sci Comput. 63:233–255.
10. Coclite GM, Garavello M, Piccoli B (2005) Traffic flow on a road network. SIAM J Math Anal. 36:1862–1886.

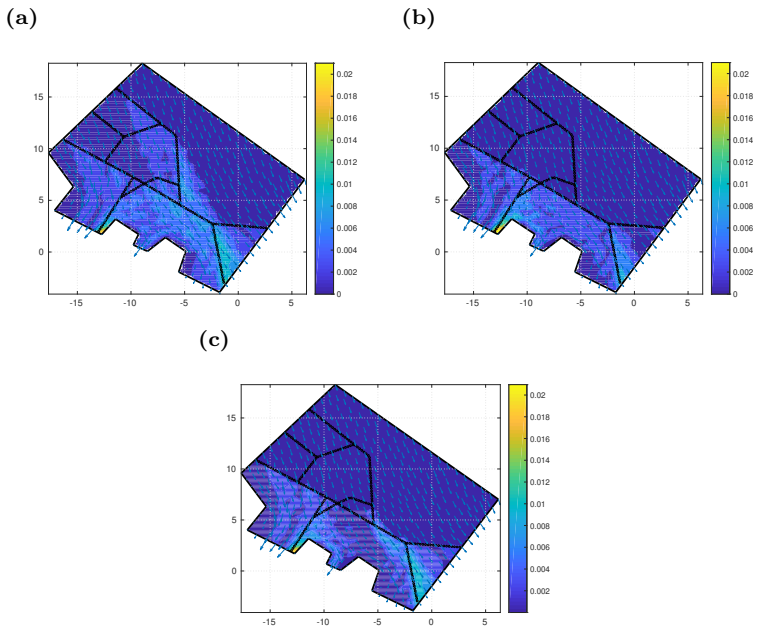

Fig. 8 Isolines for the time-averaged pollution concentration for non-optimal case **a**, relaxed Stackelberg **b** and restrictive Stackelberg **c** obtained from the numerical resolution of model (4)

11. Coclite GM, Garavello M, Spinolo LV (2017) A mathematical model for piracy control and police response. Nonlinear Differ Equ Appl. 24:24–48.
12. Deb K (2000) An efficient constraint handling method for genetic algorithms. Comput Methods Appl Mech Engrg. 186:311–338.
13. Garavello M, Piccoli B (2009) Conservation laws on complex networks. Ann I H Poincare. 26:1925–1951.
14. Garavello M, Han K, Piccoli B (2016) Models for Vehicular Traffic on Networks. American Institute of Mathematical Sciences, Springfield.
15. García-Chan N, Alvarez-Vázquez LJ, Martínez A, M.E. Vázquez-Méndez (2014) On optimal location and management of a new industrial plant: Numerical simulation and control. J Franklin Institute. 351:1356–1371.
16. García-Chan N, Alvarez-Vázquez LJ, Martínez A, M.E. Vázquez-Méndez (2017) Numerical simulation for evaluating the effect of traffic restrictions on urban air pollution. In: Quintela P, Barral P, Dolores Gómez D, et al Progress in Industrial Mathematics at ECMI 2016 edn. Springer, Cham pp 367–373.
17. Geuzaine C, Remacle JF (2009) Gmsh: a three-dimensional finite element mesh generator with built-in pre- and post-processing facilities. Int J Numer Meth Eng. 79:1309-1331.
18. Goatin P, Gottlich S, Kolb O (2016) Speed limit and ramp meter control for traffic flow networks. Eng Optim. 48:1121–1144.
19. Goldberg DE (1989) Genetic algorithms in search, optimization and machine learning. Addison Wesley Longman, Boston.
20. Gottlich S, Kuhn S, Ohst JP, et al (2011) Evacuation dynamics influenced by spreading hazardous material. Net Heterog Media. 6:443–464.
21. Gottlich S, Herty M, Ziegler U (2015) Modeling and optimizing traffic light settings in road networks. Comput Oper Res. 55:36–51.
22. Gugat M, Herty M, Klar A, et al (2005) Optimal control for traffic flow networks. J Optim Theory Appl. 126:589–616.

23. Holden H, Risebro NH (1995) A mathematical model of traffic flow on a network of unidirectional roads. SIAM J Math Anal. 26:999–1017 (1995).
24. Invernizzi G, Ruprecht A, Mazza R, et al (2011) Measurement of black carbon concentration as an indicator of air quality benefits of traffic restriction policies within the ecopass zone in Milan, Italy. Atmos Environ. 45:3522–3527.
25. Julien LA, Tricou F (2012) Market price mechanisms and Stackelberg general equilibria: an example. Bull Econ Res. 64:239–252.
26. Marchuk GI (1986) Mathematical Models in Environmental Problems. Elsevier, New York.
27. Martínez A, Vázquez-Méndez ME, Muñoz R, et al (2017) A local regularity result for Neumann parabolic problems with nonsmooth data. Indagat Math. 28:494–515.
28. Mertens J et al (2020) The Need for Cooperative Automated Driving. Electronics, 9:754. doi: 10.3390/electronics 9050754.
29. Ladyzenskaja OA, Solonnikov VA, Uralceva NN (1969) Linear and quasilinear equations of parabolic type. American Mathematical Society, Providence.
30. Orun A, Elizondo D, Goodyer E, et al (2018) Use of Bayesian inference method to model vehicular air pollution in local urban areas. Transport Res D-TR E. 63:236–243.
31. Parra-Guevara D, Skiba YN (2003) Elements of the mathematical modeling in the control of pollutants emissions. Ecol Model. 167:263–275.
32. Pestana-Barros C, Dieke PUC (2008) Choice valuation of traffic restrictions: Noise, pollution, and congestion preferences. Transport Res D-TR E. 13:347–350.
33. Shahab, Q (2012) Supporting Behavior Change in Cooperative Driving. Comm Com Inf Sc. 323-327. doi:10.1007/978-3-642-31479-755.
34. Skiba YN, Parra-Guevara D (2013) Control of emission rates. Atmosfera. 26:379–400.
35. Stockie JM (2011) The mathematics of atmospheric dispersion modeling. SIAM Review. 53:349–372.
36. Treiber M, Kesting A (2013) Traffic flow dynamics. Data, Models and Simulation. Springer-Verlag, Heidenberg-Berlin.
37. Vázquez-Méndez ME, Alvarez-Vázquez LJ, García-Chan N, A Martínez (2019) Optimal management of an urban road network with an environmental perspective. Comput Math Appl.77:1786–1797.
38. Stackelberg HV (1952) The Theory of Market Economy. Oxford University Press, Oxford.
39. Waltz RA, Morales JL, Nocedal J, et al (2006) An interior algorithm for nonlinear optimization that combines line search and trust region steps. Math Program Ser A. 107:391–408.